[10] C. Mahaim, P.-A. Carrupt, J.-P. Hagenbuch, A. Florey, P. Vogel, *Helv. Chim. Acta 63* (1980) 1149; H. Hart, N. Raja, M. A. Meador, D. L. Ward, *J. Org. Chem. 48* (1983) 4357.
[11] S. L. Miller, L. E. Orgel: *The Origin of Life on the Earth,* Prentice-Hall, Englewood Cliffs, New Jersey, USA 1974; for a contemporary view on the origin of life, see G. Wächtershäuser, *Microbiol. Rev. 52* (1988) 452.
[12] A. Eschenmoser, *Angew. Chem. Int. Ed. Engl. 27* (1988) 5; *Angew. Chem. 100* (1988) 5.
[13] J. F. Stoddart, *Nature London 334* (1988) 10.
[14] J.-M. Lehn, A. Rigault, J. Siegel, J. Harrowfield, B. Chevier, D. Moras, *Proc. Nat. Acad. Sci. USA 84* (1987) 2565; J.-M. Lehn, A. Rigault, *Angew. Chem. Int. Ed. Engl. 27* (1988) 1095; *Angew. Chem. 100* (1988) 1121.
[15] M. A. F. Elmosalamy, G. J. Moody, J. D. R. Thomas, F. H. Kohnke, J. F. Stoddart, *Anal. Proc. London 26* (1989) 12.
[16] G. G. Guilbault, J. Ngeh-Ngwainbi in G. G. Guilbault, M. Mascini (Eds.): *Analytical Uses of Immobilised Biological Compounds for Detection, Medical, and Industrial Uses (NATO ASI Ser., Ser. C; Math. Phys. Sci. Vol. 226)* Reidel, Lancaster 1988, p. 187.
[17] S. K. Burley, G. A. Petsko, *Science Washington DC 229* (1985) 23; *J. Am. Chem. Soc. 108* (1986) 7995.
[18] P. R. Ashton, N. S. Isaacs, F. H. Kohnke, A. M. Z. Slawin, C. M. Spencer, J. F. Stoddart, D. J. Williams, *Angew. Chem. Int. Ed. Engl. 27* (1988) 966; *Angew. Chem. 100* (1988) 981.
[19] R. W. Alder, R. B. Sessions, *J. Chem. Soc. Perkin Trans. 2 (1985)* 1849.
[20] A. T. Balaban, *Pure Appl. Chem. 52* (1980) 1409.
[21] D. J. Cram, S. Karbach, Y. H. Kim, L. Baczynskyj, K. Marti, R. M. Sampson, G. W. Kalleymeyn, *J. Am. Chem. Soc. 110* (1988) 2554.
[22] J. C. Sherman, D. J. Cram, *J. Am. Chem. Soc. 111* (1989) 4527; see also M. W. Browne, *The New York Times,* 21 March 1989.
[23] Z. Blum, S. Lidin, *Acta Chem. Scand. B42* (1988) 332.
[24] H. W. Kroto, *Science Washington DC 242* (1988) 1139.
[25] J.-M. Lehn, *Angew. Chem. Int. Ed. Engl. 27* (1988) 89; *Angew. Chem. 100* (1988) 91.
[26] P. Mitchell, *FEBS Lett. 176* (1984) 287.

Metal Organic Chemical Vapor Deposition (MOCVD) Perspectives and Prospects**

High Purity Semiconductors
Heteroepitaxy
Low-Dimensional Structures
Precursors for III–V Growth
Electronic Ceramics
Thin Films

By John O. Williams*

1. Introduction

This paper reviews the progress that has been made over the past decade in the use of metal organic chemical vapor deposition (MOCVD) for the preparation of high purity, epitaxial layers of a wide range of semiconductor materials: it also considers an extension of the technique to the preparation of thin film electronic ceramics and archetypal high temperature oxide superconductors.

It is now over a decade since the pioneering work of *Manasevit* and coworkers[1, 2] gave rise to the remarkable interest subsequently shown in processes that use metal-organic compounds for the production of semiconductor materials. Since 1981 four international conferences have been held on the topic,[3] numerous workshops have been organized and nowadays, for certain key III–V materials systems (and to a lesser extent narrow band gap II–VI analogs), MOCVD or metal organic vapor phase epitaxy (MOVPE) is an accepted production technique yielding novel electronic and optoelectronic devices.[4–6] In many of these cases, MOVPE compares favorably with molecular beam epitaxy (MBE) and for certain materials particularly those containing phosphorus, MOVPE can produce superior materials. MOVPE is capable of producing thin layered structures – the so-called quantum wells and superlattices – and the technique can be used for atomic layer epitaxy (ALE)[7] and in the preparation of layered crystals (LC).[8]

One area where MOCVD has not developed to the same extent as MBE is the in situ monitoring of the deposition reactions. Despite recent progress[9, 10] our understanding of the basic processes occurring in MOCVD is not very advanced and monitoring techniques are only currently being developed unlike in the case of, for example, reflection high energy electron diffraction (RHEED) in MBE to monitor and control atomic layer deposition.[11] In addition, since compounds are used as precursors in MOCVD, a great effort has to be expended in order to achieve the required levels of high purity and safety/convenience of the growth process. Many innovative preparation and purification routes have been developed[12, 13] for the most common precursors and over the past two years, safer and less toxic chemicals have been studied as alternative starting materials.[14, 15] With an improved understanding of the growth mechanisms, we can look forward to a period of considerable innovation in the use of the MOCVD technique and it is interesting to note

---

[*] Prof. J. O. Williams
Solid State Chemistry Group
Department of Chemistry
UMIST, PO Box 88
Manchester M60 1QD (UK)

[**] I would like to thank members of the UMIST Solid State Chemistry Group and the UK JOERS Consortium on InP-based materials for numerous stimulating discussions. The financial support of the SERC, US Air Force, Thorn EMI CRL, Air Products Ltd. and Johnson Matthey Ltd. is also gratefully acknowledged.

that this is already happening in the fields of both electronic ceramics e.g. $PbTiO_3$[16, 17] and high-T_c oxide superconductors of the family $YBa_2Cu_3O_x$ (x:6 to 7).[18, 19]

2. Attainment of High Purity in Semiconductor Materials

Most advances in semiconductor devices rely on the availability and subsequent doping of high purity materials. In recent years there have been significant advances in this field. MOCVD has its own difficulties in this area additional to those of other conventional preparative techniques since the precursors that are used do not lend themselves to ready purification: they are often pyrophoric, hazardous chemicals. It is now possible to analyze directly the metal organic precursors for elemental impurities at the ppb level using variants of inductively coupled plasma (ICP) analysis.[20]

Parallel studies to characterize impurities in the grown epitaxial layers by such techniques as secondary ion mass spectrometry (SIMS) and low temperature photoluminescence (PL) allow correlation between impurities in the starting materials and those in the epitaxial layers.[21–23] This relationship may be illustrated by reference to some recent work on the growth of GaAs. Two batches of trimethyl gallium (TMGa) were used with the same, high purity, arsine source. The ICP analysis of the TMGa showed different amounts of common impurities as shown in Table 1. The level of Si and Zn, recognized n- and p-type impurities respectively in GaAs, is lower in source TMGa2 than in TMGa1. The electrical characteristics of GaAs grown from TMGa2 and arsine are much improved over those from TMGa1 and the same arsine. The low temperature (77 K) electron mobility and concentration are higher and lower, respectively, and for TMGa2 the lowest carrier concentration and highest mobility are obtained at the lower growth temperature of 600 °C (Figure 1). This low growth temperature can

Table 1. ICP analysis for impurities in TMGa1 and TMGa2*.

Elements	TMGa1	TMGa2
Si	0.2 ppm	0.05 ppm ND
Zn	0.6 ppm	0.3 ppm ND
Sn	< 0.5 ppm ND	0.5 ppm ND
Mg	0.05 ppm	0.05 ppm ND
Mn	< 0.05 ppm ND	0.05 ppm ND
Fe	< 0.3 ppm ND	0.3 ppm ND

* ND = not detected

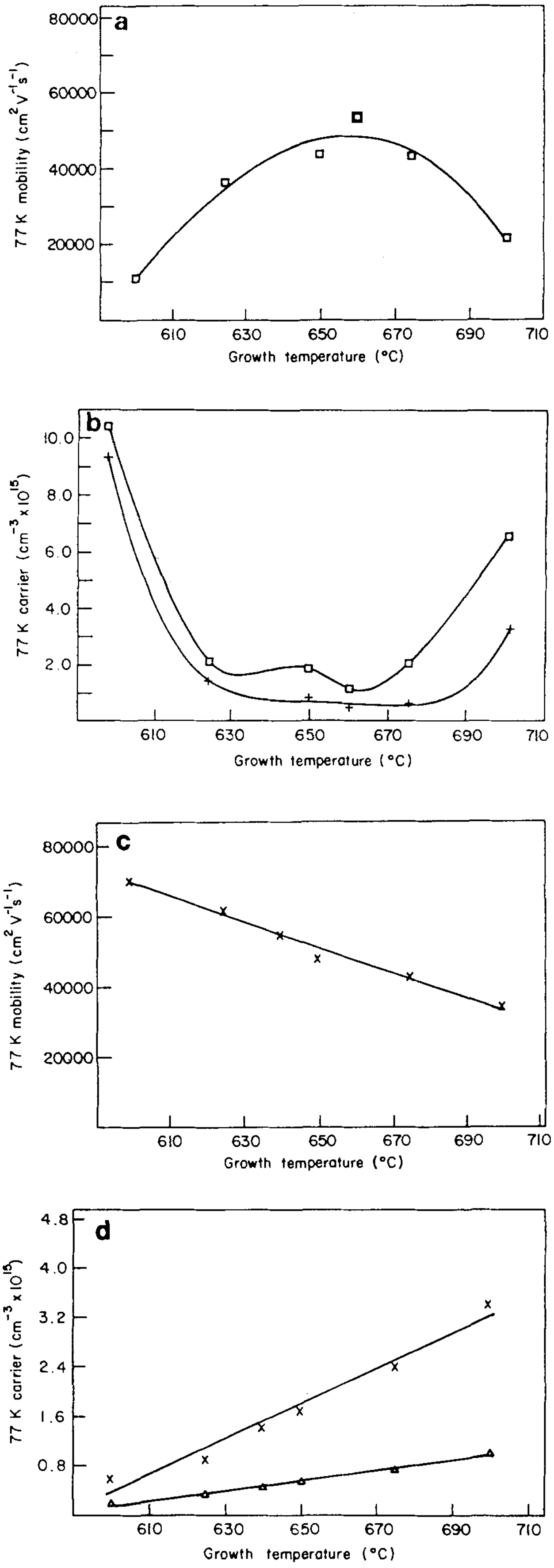

Fig. 1. a) 77 K Hall mobility variation with growth temperature for GaAs grown from TMGa1 at constant V/III ratio of 75:1. b) 77 K Hall carrier concentration yielding values of (□) N_D and (+) N_A plotted against growth temperature for GaAs grown from TMGa1 at constant V/III ratio of 75:1. c) 77 K Hall mobility variation with growth temperature for GaAs grown from TMGa2 at constant V/III ratio of 75:1. d) 77 K Hall carrier concentration yielding values of (X) N_D and (△) N_A plotted against growth temperature for GaAs grown from TMGa2 at constant V/III ratio of 75:1.

be adventitious for good morphology and crystallinity of the epilayers. The electrical properties are dominated by the Si and the activated incorporation of this impurity is consistent with doping studies using disilane.[24]

A similar situation is observed in the case of InP preparation by MOCVD where Si is again found to be the dominant impurity in the highly purified organometallic precursor, trimethylindium (TMIn). The presence of this impurity in the grown layers has been confirmed by depth profiling studies and analysis of low temperature photoluminescence spectra.[21] Figure 2a shows the electron concentration as a function of depth through the InP epilayers grown with increasing temperatures. The corresponding silicon profile in SIMS is shown in Figure 2b. Low temperature (4 K) PL spectra confirm the presence of donors, and measurements in a magnetic field (where the donor related transitions are resolved) indicate the presence of S and Ge impurities in addition to the Si. Removal of Si yields extremely high quality InP material with theoretical values of electron mobility and concentration reached for epilayers ca. 10 µm in thickness. Indeed, one of the highest reported electron mobility values for InP ca. 400.000 cm^2 V^{-1} at 60 K has been reported for MOCVD material using purified TMIn.[25] The two examples cited are for binary materials. There have also, as a result of this success with GaAs and InP, been significant improvements in the purity of ternary and quaternary materials. This will not be covered in this review, but the interested reader is referred to the recent literature.[26]

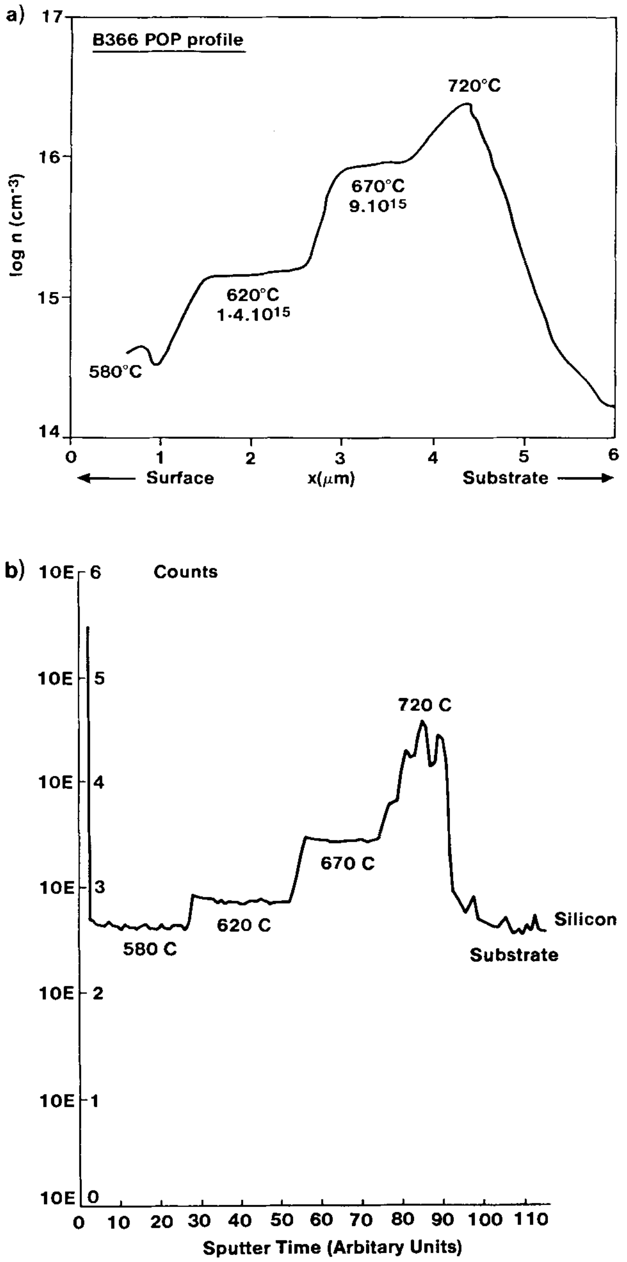

Fig. 2. a) Undoped MOCVD InP-variation of doping level with growth temperature. b) Undoped MOCVD InP-variation of silicon content with growth temperature (SIMS Profile).

3. Heteroepitaxy

Heteroepitaxy describes the situation where an epitaxial layer of one material is grown upon another in strict crystallographic registry. In addition to providing considerable fundamental scientific interest such materials combinations have enormous technological significance. Table 2 summarizes the properties of a few simple heteroepitaxial systems which are prepared by MOCVD. The list is confined to binary and elemental materials although, as we shall see later in sections 4 and 5, systems including ternary and quaternary materials may also be classified as heteroepitaxial.

Table 2. Simple heteroepitaxial systems.

Material	Crystal Structures	Unit Cell dimension a_0/pm	Lattice Mismatch $[\Delta a/a]_0$ $\times 10^2$	Band Gap /eV
GaAs (e)	sphalerite (fcc)	0.565331	+4.09	1.35
Si (s)	diamond	0.543072		1.14
GaAs (e)	sphalerite (fcc)	0.565331	−3.68	1.35
InP (s)	sphalerite	0.586928		1.29
ZnSe (e)	sphalerite (fcc)	0.56670	+0.24	2.67
GaAs (s)	sphalerite (fcc)	0.565331		1.35

(e) epitaxial layer; (fcc) face-centered cubic; (s) substrate: $[\Delta a/a]_0$ is the measurement for a stress free epitaxial layer and is defined as $(a_0 - a_s)/a_s$ where a_s is the unit cell dimension of the substrate.

It is instructive to consider these pairs of materials in turn. Since Si dominates the commercial semiconductor market, there has been interest in preparing GaAs on Si. There appear to be significant advantages if this could be done properly including: the relative cheapness of Si substrates as compared to GaAs, the better thermal conductivity of Si with relevance to power devices, the ability to combine high speed GaAs devices with high density Si circuits and the possibility for fabrication of GaAs opto-electronic devices in combination with Si integrated circuits. However, two major difficulties arise. First the two materials differ in the symmetry of their respective crystal structures, and second, the unit cell dimensions differ leading to a "lattice mismatch" at the interface between epilayer and substrate. The symmetry difference (sometimes referred to as different color symmetry) leads to the formation of anti-phase boundaries (APB) when growth proceeds on substrate surfaces of particular orientations with catastrophic consequences for electrical behavior at the interfaces. Because of these difficulties it is now accepted that any devices made in the GaAs/Si system and relying on the GaAs must utilize material well away from the interface unless the APBs and other defects can be eliminated. Furthermore, these limitations are likely to preclude the development of devices that utilize both Si and GaAs simultaneously. Considerable progress has been made recently in the MOCVD growth of GaAs on Si without necessarily employing buffer layers to accommodate the lattice mismatch.

Preparation of Si surfaces prior to growth is a prerequisite and a complex series of nucleation and crystal growth steps appear necessary for the preparation of GaAs with acceptable crystallinity. Figure 3 illustrates how surface preparation, nucleation and growth temperature affect the crystallinity of GaAs grown on accurately oriented (100)Si substrates. Experiments to reduce interfacial defects have also been carried out employing substrate surfaces deviating from (100) orientation and good properties obtained at 4° off towards (110).[27] In addition to the problems encountered in the GaAs/Si system the other two pairs of materials referred to in Table 2 suffer the disadvantage of possible interdiffusion of elements with catastrophic consequences if it occurs to an appreciable extent. The situation is worst for ZnSe/GaAs since Zn acts as a p-type dopant in GaAs and Ga as an n-type dopant in ZnSe. Excellent quality ZnSe has been grown on (100)GaAs surfaces by reduced and atmospheric pressure MOVPE.[28] Room temperature photoluminescence is observed indicating the low concentrations of shallow and deep centers, but the structural, electrical and optical properties are highly dependent on epilayer thickness and the distance away from the interface. The X-ray and PL data for ZnSe epilayers grown on GaAs and varying in thickness from 0.5 µm to 8.0 µm are given in Figure 4. In the thinnest layers, deep center emission appears in the PL and in the X-ray data the ZnSe diffraction maxima are shifted to lower 2θ values. SIMS analysis on the ZnSe reveals the presence of Ga diffusion from the substrate (Fig. 4c) and cross sectional transmission electron microscopy (Fig. 4d) confirms the defective nature of the interface. It is unlikely that the ZnSe/GaAs interface can be made sufficiently good to support efficient devices relying on optical/electronic properties. However, the ternary $ZnSe_{0.95}S_{0.05}$ grown on GaAs[29] offers a lattice-matched system, and studies following MOCVD growth indicate that its properties are superior to those of ZnSe/GaAs and adequate to support devices. The distortion at the interface of ZnSe/GaAs renders the structure tetragonal as opposed to cubic[30] and this has been

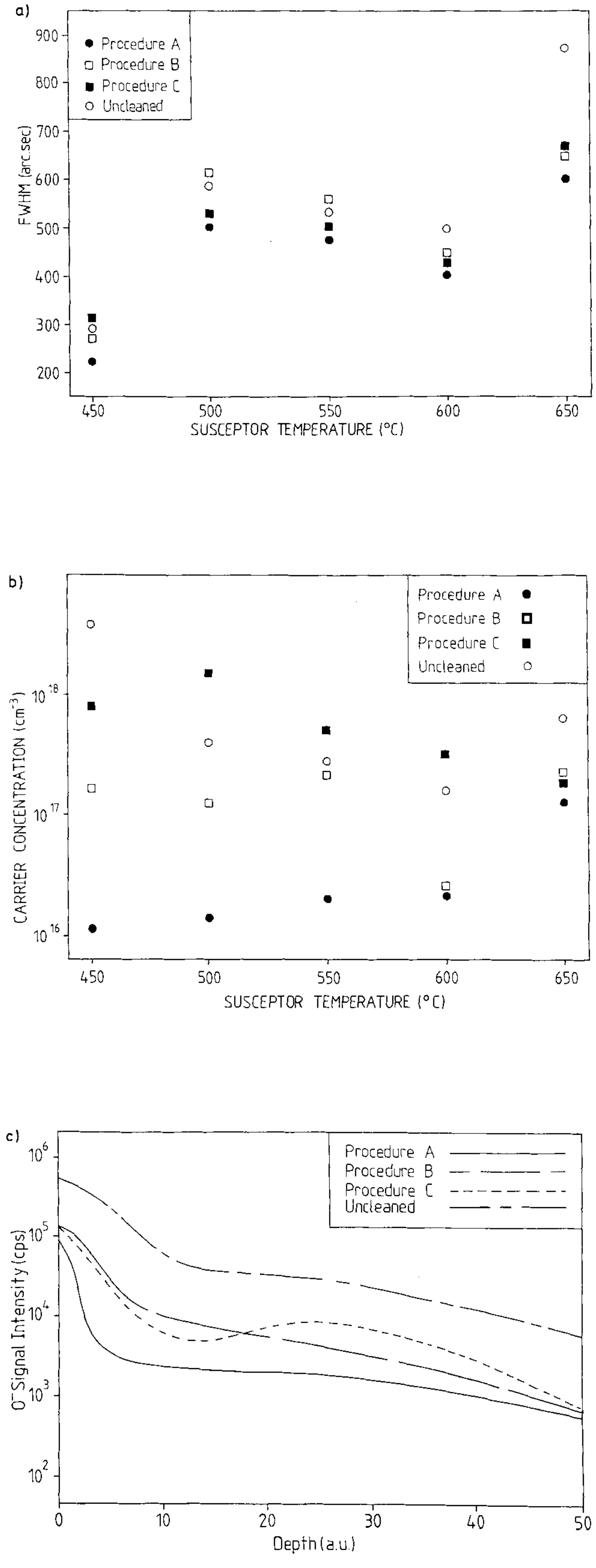

Fig. 3. a) X-Ray rocking half widths vs. susceptor temperature for each Si(100) surface. b) Background carrier (electron) concentration vs. susceptor temperature. c) Dynamic SIMS spectra showing surface oxide thickness for each Si(100) surface.

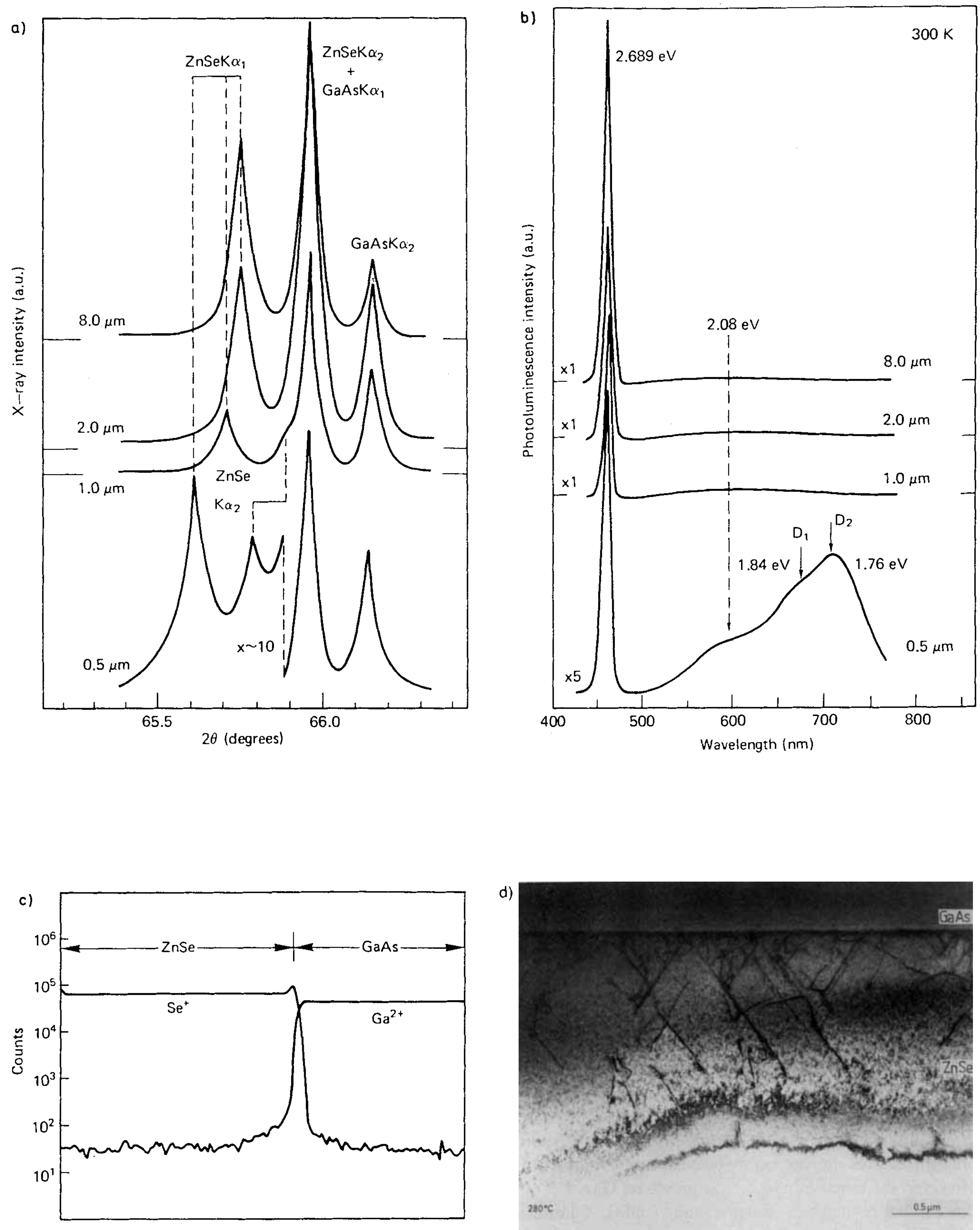

Fig. 4. a) Variation of X-ray rocking curve data for ZnSe/GaAs with layer thickness. b) Variation of 300 K PL spectra for ZnSe/GaAs with layer thickness. c) Secondary ion mass spectrometry (SIMS) profiles for $Se^{\oplus}$ and $Ga^{2\oplus}$ in ZnSe/GaAs. Note the tail in the $Ga^{2\oplus}$ profile. d) Cross-sectional TEM for ZnSe/GaAs grown by MOVPE at 280 °C showing dislocation structure close to the interface.

confirmed recently by electron spin resonance studies of Mn-doped ZnSe using the $Mn^{2\oplus}$ ions to probe the local symmetry.[31]

GaAs has been grown successfully on InP substrates[32] and efficient devices such as solar cells and MESFETS have been fabricated. As with the other two heteroepitaxial systems these do not rely on charge carrier transport across the interface or on optical generation of carriers in that region. We can, therefore, conclude that in these three heteroepitaxial systems we have important building blocks for the development of integrated opto-electronic devices that will combine important electronic and optical functions on a common substrate i.e. Si, GaAs or InP.

4. Ternary and Quaternary Materials

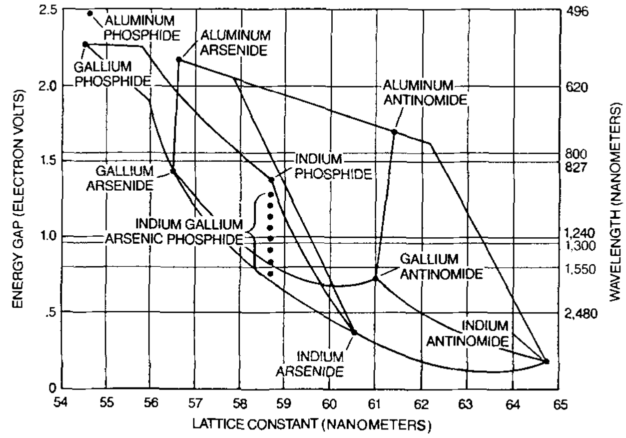

Fig. 5. Band-gap engineering of a semiconductor can be done by varying the elemental components of the semiconductor alloy in a controlled way. Here the energy across the band gap is plotted against the lattice constant, or the dimension of the basic unit of the crystalline lattice. The lines that connect points on the graph show how the band gap and the lattice constant vary for mixtures of the binary compounds to which the points correspond. Such mixtures are ternary compounds. For example, the ternary compound gallium aluminum arsenide can be made to have any band gap between about 1.4 and 2.2 electron volts by varying the ratio of gallium to aluminum between the band-gap extremes represented by gallium arsenide and aluminum arsenide. Materials of differing composition that have roughly the same lattice constant, such as these two binary compounds, can be deposited in alternating layers to create a single crystal lattice. Operating wavelengths for three important optical communications systems are 800, 1300 and 1550 nm [55].

Figure 5 shows how the band gap of III–V materials varies with the lattice constant and composition. Such diagrams are often referred to as phase diagrams and they aid the crystal grower in his choice of material system appropriate to a particular electronic/optical requirement. (The term band gap engineering is commonly used to describe this approach). The tie-lines represent ternary compositions e.g., $Ga_{1-x}In_xAs$ and $InAs_{1-y}P_y$ and areas on the diagram contained within points of four binary compounds represent quaternary materials e.g., $Ga_{1-x}In_xAs_{1-y}P_y$. It is apparent that one particular ternary composition will have the same lattice constant as a binary compound and this may be found by drawing vertical lines through the binary point to intercept the tie-line for that particular ternary e.g. $Ga_{0.47}In_{0.35}As$ is lattice matched to InP (dotted line). Similarly, a range of quaternary compositions e.g. $Ga_{1-x}In_xAs_{1-y}P_y$ with $0 < x < 1$ and $0 < y < 1$ will be matched to InP and will be represented by the same vertical dotted line. Almost the entire range of III–V direct band gap, ternary and quaternary materials have been prepared by MOCVD. For many of these the problem of compositional uniformity both within the bulk and across the surface of the grown layers has been solved and lattice matching is achieved with good morphology and crystallinity of the grown layers. One of the most important III–V ternary systems is $Ga_{1-x}Al_xAs/GaAs$ and the other is $Ga_{1-x}In_xAs/InP$. The "AlGaAs" system is unique in that lattice-matching to GaAs is retained for a wide range of x values since the radii of Al (1.43 Å) and Ga (1.41 Å) are similar. In contrast only one composition of "InGaAs" is lattice-matched to InP. Double crystal X-ray rocking curve analysis confirms that a

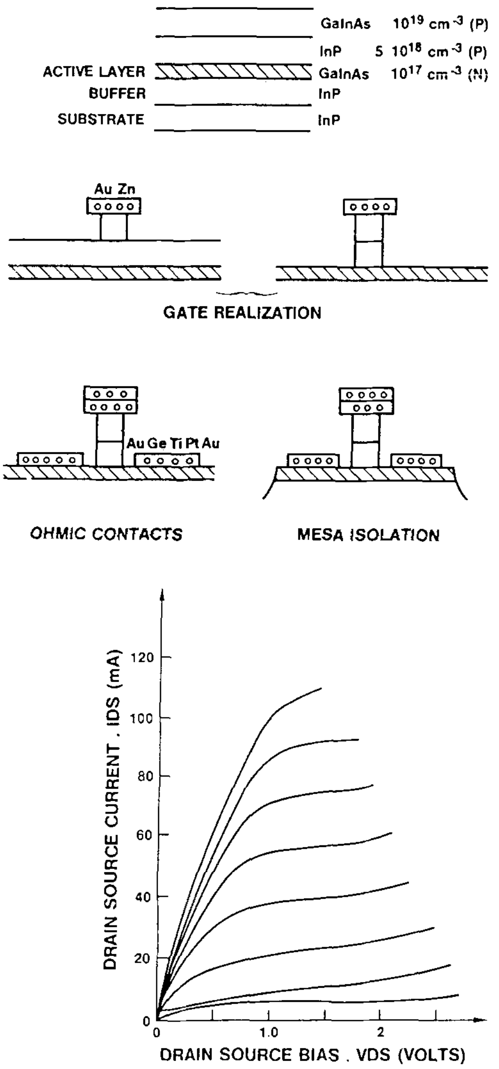

Fig. 6. (Top) Schematic diagram of the JFET fabrication process. (Bottom) JFET DC characteristics.

lattice mismatch $[\Delta a/a]_0$ of less than 8×10^{-5} may be routinely obtained with a full width at half maximum (FWHM) of < 40 arc/sec for this system. Several device structures including junction field effect transistors (JFETs) and double heterostructure pindiodes have been fabricated with excellent characteristics. Figure 6 gives details of the structure, fabrication, uniformity and characteristics of a typical JFET structure grown by MOCVD.[33]

The quaternary system $Ga_{1-x}In_xAs_{1-y}P_y$ covering the entire composition range has also been prepared by MOCVD[34] and the field has been reviewed recently.[6] There are also important advances presently being made with ternary and quaternary materials containing antimony.[35]

Over the past three years, *Dupuis* and collaborators have made significant advances in the fabrication of low threshold, high efficiency $Al_{1-x}Ga_xAs$/GaAs double heterostructure injection lasers directly on Si substrates.[36] As mentioned in section 3, this is another example of heteroepitaxy but in this work, the lattice mismatch has been accommodated by the preparation of Si/Ge buffer layers. Four types grown by MBE have been used (i) single Ge layers (1 µm thick) deposited on Si (ii) a single Ge layer grown on Ge/Si strained layer superlattice, (iii) a Ge layer deposited on linearly graded Ge/Si alloy buffer layer, (iv) a combination of (ii) and (iii). It is found that the best device performance is obtained using procedure (i)[37] and this work illustrates the sophistication of layered structures that can be prepared by a combination of MBE and MOCVD.

5. Low-Dimensional Structures and Devices

Over the past decade there has been considerable progress in the study of low dimensional structures prepared by both MOCVD and MBE. It is not my intention in this review to compare the two techniques and the task of presenting a comprehensive account of 'LDS/LDD' is an impossible one because of the enormity of the subject area. I shall, therefore, be highly selective in my choice of topics and will attempt to address particular materials problems. The interested reader is referred to three recent excellent reviews which cover other aspects.[38, 39, 54]

Initial studies dealt with the "AlGaAs/AlAs" or "AlAs/GaAs" quantum well and multiple quantum well structures. Here GaAs acts as the well material and AlAs or AlGaAs as the material in the barrier layers. Lasers operating in the red spectral region ca. 850 nm are now in commercial use. A particularly interesting structure is that of a graded refractive index separate confinement heterostructure single quantum well laser (GRINSCH SQW laser). The laser consists of a 500 nm GaAs buffer layer, 1 µm $Al_{0.6}Ga_{0.4}As$ cladding, 340 nm graded "AlGaAs" confinement region within an 8 nm thick GaAs SQW active layer, 500 nm $Al_{0.6}Ga_{0.4}As$ cladding and 100 nm GaAs contact layer. This type of laser gives continuous wave (CW) operation at room temperature with a broad area threshold current density of ca. 300 Acm^{-2} and a single longitudinal mode operation at 843 nm with a peak width of less than 1 nm.[32]

The advent of devices such as high electron mobility transistors (HEMTs) based on a two dimensional electron gas (2 DEG) formed in the "AlGaAs"/GaAs system has further emphasized the dimensionality of these thin layer structures. Figure 7a is a schematic diagram of a typical heterojunction structure grown by MOCVD. The two dimensional electron gas is formed in the undoped GaAs layer just below the thin ca. 15 Å undoped "AlGaAs" layer and sustains a high electron mobility in two dimensions (Figure 7b). The doping in the upper "AlGaAs" layer is achieved using selenium. A

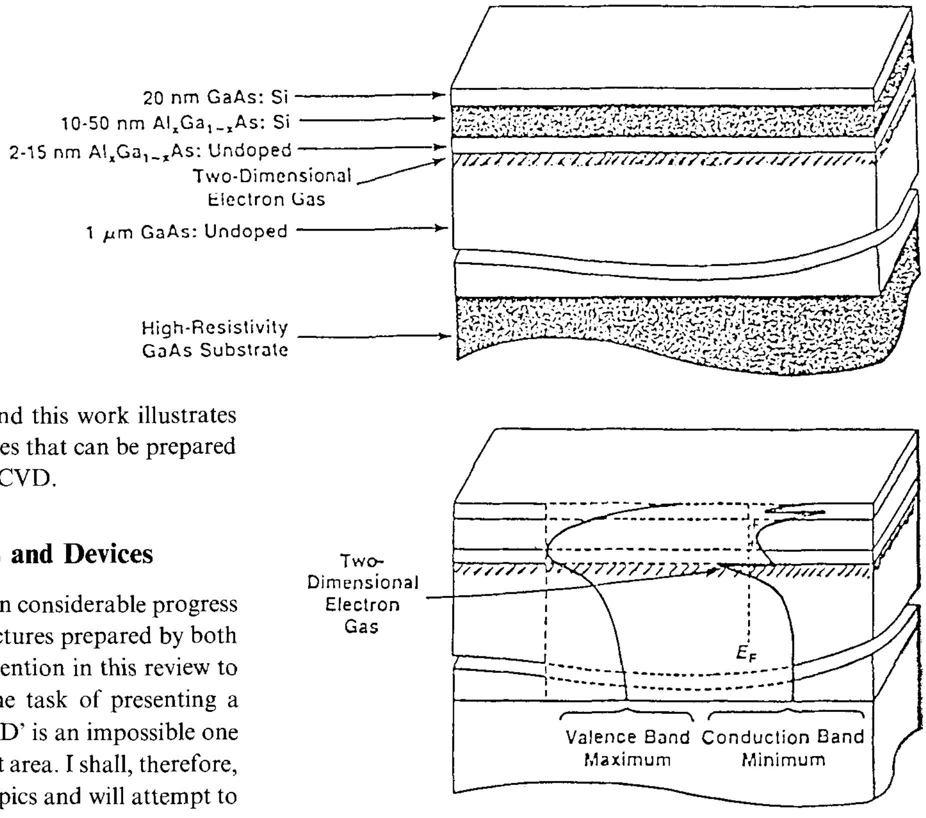

Fig. 7. a) Cross section of a modulation doped heterojunction. b) Energy band diagram for structure of (a). The two dimensional electron gas formed in the structure is ideal for the conducting channel of a FET.

HEMT structure requires good doping uniformity, low carrier concentration in undoped material and sharp interfaces. These requirements can be met by MOCVD. Multiple quantum well structures in InP-based ternary and quaternary materials have also been prepared by MOCVD. Figure 8 shows the actual structure grown and the corresponding photoluminescence spectra for the GaInAsP/InP system. It should be noted that each quaternary well yields a PL emission peak which shifts to lower wavelengths as the well width decreases.

Examination of Figure 8 allows us to understand the concept of strained layer superlattices (SLS) and pseudomorphic structures. It has been shown that dislocations in ternary materials grown on binary semiconductors can be confined to the interfacial regions when the layers are thin ca. ≤ 200 Å.

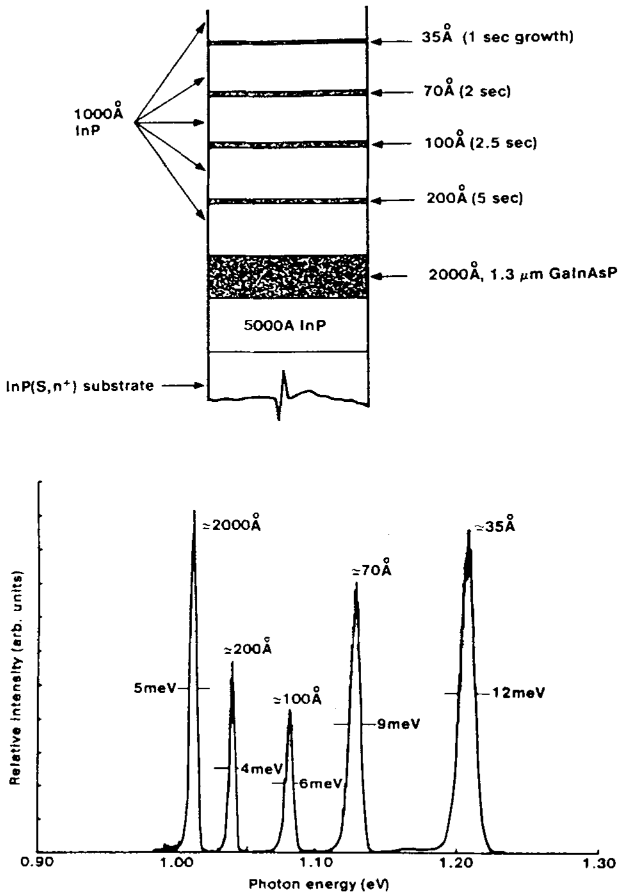

Fig. 8. a) GaInAsP/InP quantum wells grown to assess epitaxy and interface quality. b) Photoluminescence spectrum of a GaInAsP multiquantum well sample, emission from each of the four different wells and from the bulk epitaxial material can be observed. $T = 4.2$ K, 25 mV, 40 mW, 0.18 W cm^{-2}.

Furthermore, the effective lattice-matched composition of the ternary can be achieved by growing successively thin layers of different binary compounds of the required thickness. Thus, the composition $Ga_{0.47}In_{0.53}As$ can be built up of GaAs and InAs layers of appropriate relative thickness. In a similar way, the quaternary of a given composition can be equivalent to two ternaries, neither of which is lattice-matched to the substrate. Typical materials combinations that have been grown successfully by MOCVD are indicated in Table 3. In order to achieve uniform compositions and sharp interfaces, careful control of reactor geometry is required.

Table 3. Typical materials combinations.

GaAs	–	$Al_{1-x}Ga_xAs$
GaAs	–	$In_{1-x}Ga_xAs$
GaAs	–	InAs
GaAs	–	$GaAs_{1-y}Sb_y$
GaAs	–	$In_{1-x}Ga_xP-In_{1-x}Al_xP$
InP	–	$In_{1-x}Al_xAs-In_{1-x}Ga_xAs$
InP	–	$In_{1-x}Ga_xAs_{1-y}P_y$
InP	–	InAs–GaAs
GaSb	–	InAs
GaSb	–	$InAs-AlAs_{1-y}Sb_y$
GaSb	–	AlSb
GaSb	–	$In_{1-x}Ga_xAs_{1-y}Sb_y-Al_{1-x}Ga_xAs_{1-y}Sb_y$

6. Novel Precursors for III–V Growth

Conventional group III organometallic and group V hydrides used as precursors for MOCVD suffer severe disadvantages despite the fact that good quality epitaxial layers can be produced in the majority of cases. These disadvantages arise from the toxic and hazardous nature of arsine and phosphine, for example, and the pyrophoric nature of TMGa and TMIn. TMIn suffers further limitations due to its crystalline nature which can severely reduce the levels of compositional uniformity that can be obtained in several ternary and quaternary systems.

Another important consideration when preparing complex systems is the relative thermal behavior of a pair of group III and/or group V precursors. Arsine and phosphine, for example, decompose in the gas phase and, as far as is known, at GaAs and InP substrate surfaces, with very different rates. Such considerations have prompted several research groups worldwide to seek alternative precursors. Table 4 lists alternative precursors for arsine that have been

Table 4. A selection of alternative As precursors used with TMGa to produce GaAs.

Compound	Vapor Pressure	GaAs n_{77K}/cm^{-3}	electrical data Ref μ_{77K}/cm^2 V^{-1} s^{-1}
Trimethylarsine (TMAs)	235 Torr at 20 °C	$p \sim 10^{17}$	–
Triethylarsine (TEAs)	5 Torr at 20 °C	$n \sim 5 \times 10^{15}$	13.000
Diethylarsine (DEAs)	0.8 Torr at 18 °C	$n \sim 3 \times 10^{14}$	64.000
Tertiarybutylarsine (TBAs)	96 Torr at –10 °C	$n \sim 1 \times 10^{15}$	53.000
Phenylarsine	2 Torr at 20 °C	$n \sim 1 \times 10^{15}$	40.000

examined in recent years for GaAs growth by MOCVD. With most of these reagents carbon incorporation is a major problem and hitherto only two precursors, tertiarybutylarsine (TBAs) and phenylarsine (PAS) have shown real promise. Both of these are liquids under normal conditions. GaAs with relatively high electron mobilities (ca. 40.000 $cm^2 V^{-1} s^{-1}$ at 77 K) and low donor concentration for nominally undoped material ($n \leq 1 \times 10^{15} cm^{-3}$) has been reported.[14] For the case of InP growth, liquid tertiarybutylphosphine (TBP) has also shown promise.[15] It may be no accident that these liquid precursors, with hydrogen atoms linked directly to the group V element, yield epitaxial layers relatively free of carbon impurities, in contrast to those precursors that contain no group V–H bonds, e.g. trimethyl- and triethylarsine (TMAs and TEAs respectively). It appears that As–H and/or As–H_2 units are required in order to react with methyl radicals from TMGa to form GaAs without resulting in carbon formation, although final details await mechanistic investigations currently underway in several laboratories. PAS is also being used to grow InAs.

From time to time in the MOCVD field, there has been interest in developing adduct precursors or "magic compounds" where the group III–group V bond has already been formed.[40] Thermal dissociation would simply detach side groups leaving behind the III–V binary compounds, a process that would be safe and cheap. However, progress in this area has been disappointing for several reasons. First, the adducts cannot be purified sufficently: second, they require the presence of other group III or group V sources in order to produce stoichiometric material and third, they cannot alone provide ternary and quaternary materials of variable composition.

7. Crystallography – Controlled Growth

The manufacture of the current generation of electronic devices with features of the order of several microns involves complex etching and lithographic processes which are both inefficient and time consuming. Therefore, considerable interest is being shown in local or selected area deposition where the semiconductor material is deposited only where it is required, e.g. in the active region. There have been several approaches to achieving selected area deposition using MOCVD. One has involved "photo-assisted" deposition using, for example, laser radiation and capitalizing on photonic or thermal effects to deposit the desired material. Several review articles have appeared covering these aspects.[41, 42] A much more recent and novel approach is to use precursors selectively to deposit on particular surfaces but not on others. The acronym CODE, compound and orientation dependent epitaxy, has been used to describe this technique.[46] Such growth surfaces would vary in their composition and/or structure and crystallography. It is also desirable to use MOCVD to overgrow contoured substrates in order to isolate component function, and for interfacing. The work of *Hersee* et al.,[43] *Demeester* et al.,[44] *Yoshikawa* et al.,[45] *Scott* et al.[46] and *Garrett* and *Thrush*[47] covering both GaAs and InP based systems should be consulted for further details. Much of this work has been concerned with the ability of MOCVD to deposit over mesa-type structures and into channels of given crystallography.

Such capabilities would assist in the fabrication of buried heterostructure lasers, waveguides and active/passive waveguide interfaces by single step epitaxy. A common technique to study the behavior over contoured substrates is to employ a multi-heterostructure growth technique to follow the time evolution of the growing surfaces, i.e. to grow a superlattice whose individual layer thickness is much less than the total thickness of the grown layer. Although the precise distortion of the growth process introduced by the creation of the superlattice is uncertain, some general preliminary conclusions can be drawn in relation to the preference for growth on certain crystallographic planes in the InGaAs/InP and AlGaAs/GaAs systems: (i) InGaAs is reluctant to nucleate on either (111)A or (111)B surfaces, whereas InP grows on all available crystal planes. AlGaAs/GaAs on the other hand nucleates on (111)A surfaces but not on (111)B surfaces. (ii) For both systems nucleation and growth on (100) and (110) surfaces appears to be better than for (111) surfaces. Clearly, the growths are controlled by surface free energies, preferential adsorption, differential sticking coefficients etc. and it will be interesting to see the results of controlled experiments involving, for example, different precursors for the group III elements.

8. Electronic Ceramics and Oxides

Over the past two years, there has been growing interest in the so-called high-T_c oxide superconductors typified by the composition $YBa_2Cu_3O_{7-x}$ where $0.1 < x < 0.2$.[48] Superconducting transition temperatures around 90 K have been obtained for compressed, polycrystalline samples prepared by sintering and annealing the constituent oxides in specific proportions. In addition, other compositions based on Bi, Tl, Sc etc. have shown promise.[49] In order to be compatible with electronic and other types of device structures and the complete range of processing technologies it is desirable to prepare these materials as thin films. There have been various reports of successes using, for example, vacuum evaporation, sputtering, MBE, spray pyrolysis and screen printing. MOCVD has also been used with variable success.[50] Hitherto, metal chelate precursors such as 2,2,6,6-tetramethyl-3,5-heptanedione (thd) derivatives have been used, but the process has been unreliable and the thermal growth has to be followed in most cases by either a high temperature treatment or an annealing process under controlled conditions. The main difficulties arise from the choice of precursor and substrate material and these have not been optimized. In general, the following conditions are typical:

(i) precursors kept at ca. 150 °C to 300 °C
(ii) substrate materials such as MgO or yttrium stabilized zirconia
(iii) growth temperatures in the range 600–900 °C
(iv) subsequent annealing in O_2 or high temperature treatment at ca. 900 °C
(v) reduced pressure operation (10–100 Torr) with heated lines from precursor containers to the growth chamber.

Thin films of "YBCO" have been obtained with preferred orientation (*c* axis normal to film plane) and variable composition, exhibiting superconducting transition temperatures over the range 30 to 80 K. Recently, we have improved the compatibility of precursors by using fluorinated β-diketones of the three metals Y, Ba and Cu and this appears also to improve the reproducibility of the MOCVD process.[51] We have demonstrated control over the composition as measured by energy dispersive X-ray analysis (EDAX) and the perovskite structure can be obtained by careful choice of processing temperature and substrate material/orientation. Future work in this area should address the understanding of the basic deposition process in order to remove the empiricism currently prevailing, and photo-assisted techniques should be investigated.

Four years ago, we proposed MOCVD routes for the preparation of electronic ceramic and ferroelectric oxides typified by $PbTiO_3$ and $Pb(La,Zr)TiO_3$. In recent years this has proven possible for $PbTiO_3$, in particular, using alkoxide and β-diketone derivatives of Pb and Ti and some success has been obtained with $Pb(La,Zr)TiO_3$. In addition, the work of *Brierley* et al.[52] using a range of precursors has demonstrated the preparation by MOCVD of $PbTiO_3$ and $Pb(Sc,Ta)O_3$ thin films. The stoichiometry and thickness of the films may be controlled by adjusting the temperatures of the precursors, the flow rate of the carrier gas and the deposition time. As with the "YBCO" system, post-growth heat treatments and/or annealing are necessary to achieve the required crystalline structure (phase). The reader could well ask what are the advantages of MOCVD for these two materials systems. The main one overcomes the inability of sputtering to maintain stoichiometry in these complex oxides and the other removes the need with spray pyrolysis to perform the deposition sequentially in order to build up film thickness. Also in this context, our experiences with laser ablation from single targets of $PbTiO_3$ and/or $Pb(La,Zr)TiO_3$ have demonstrated that it is extremely difficult to retain film stoichiometry and obtain the pervoskite phase.[53]

9. Conclusion

In this review, I have attempted to cover certain materials aspects of MOCVD. What is readily apparent is the tremendous versatility of the MOCVD processes and their applicability to the preparation of a wide range of important materials systems. Thin film epitaxial structures of widely varying but controlled compositions and thicknesses can be prepared with complete certainty and we appear to be confined at present only by the limited range and purity of available precursors. We are also beginning to understand the fundamentals of the growth processes that involve complex combinations of gas phase and surface phenomena. Progress in this area will remove the empiricism currently dominating our quest for better and novel starting materials. The entire field appears to have an exciting future and should contribute to the development of advanced materials for many years to come.

Received: June 14, 1989

---

[1] H. M. Manasvelt, *Appl. Phys. Lett. 12* (1968) 136.
[2] H. M. Manasvelt, W. I. Simpson, *J. Electrochem. Soc. 116* (1969) 1725.
[3] a) ICMOVPE-I Ajaccio, France 1981, *J. Cryst. Growth 55* (1981). b) ICMOVPE-II Sheffield, England 1984, *J. Cryst. Growth 68* (1984). c) ICMOVPE-III California, USA 1986, *J. Cryst. Growth 77* (1986). d) ICMOVPE-IV, Hakone, Japan 1988, *J. Cryst. Growth 93* (1988).
[4] P. D. Dapkus, *J. Cryst. Growth 68* (1984) 345.
[5] P. H. Manuel, M. Defour, C. Grattepain, F. Omnes, O. Archer, G. Timms, M. Razeghi, *Chemtronics 4* (1989) 40.
[6] M. Razeghi: *The MOCVD Challenge,* Vol. 1, A. Hilger, Bristol 1989.
[7] H. Sasaki, M. Tanaka, J. Yoshino, *Jpn. J. Appl. Phys. 24* (1985) 417.
[8] T. Fukui, H. Saito, *Jpn. J. Appl. Phys. 24* (1985) L774.
[9] R. Luckerath, P. Balk, M. Fischer, D. Grundmann, A. Hertling, W. Richter, *Chemtronics 2* (1987) 199.
[10] J. O. Williams, R. D. Hoare, M. J. Parrott, *Phil. Trans. R. Soc. (Lond.)* 1989, in press.
[11] B. A. Joyce in P. M. Dryburgh, B. Cockayne, K. G. Barraclough, (Eds.): *Advanced Crystal Growth,* Prentice Hall 1987, p. 337.
[12] A. H. Moore, M. D. Scott, J. I. Davies, D. C. Bradley, M. M. Faktor, H. Chudzynska, *J. Cryst. Growth 47* (1989) 15.
[13] A. C. Jones, *Chemtronics 4* (1989) 15.
[14] G. T. Muhr, D. A. Bohling, T. R. Omsbead, S. Brandon, K. F. Jensen, *Chemtronics 4* (1989) 26.
[15] G. B. Stringfellow, *J. Electron. Mater. 17 (4)* (1988) 327.
[16] J. O. Williams, B. Gould, unpublished results.
[17] C. J. Brierley, C. Trundle, L. Considine, R. W. Whatmore, F. W. Ainger, private communication.
[18] J. O. Williams, N. I. Dunhill, unpublished results.
[19] H. Yamane, H. Kurosawa, H. Iwasaki, H. Masumoto, T. Hirai, N. Kobayashi, Y. Muto, *Jpn. J. Appl. Phys. 27 (7)* (1988) L1275.
[20] A. C. Jones, G. Wales, P. J. Wright, P. E. Oliver, *Chemtronics 2* (1987) 83.
[21] N. D. Gerrard, D. J. Nicholas, J. O. Williams, A. C. Jones, *Chemtronics 3* (1988) 17.
[22] N. Hunt, J. O. Williams, *Chemtronics 2* (1987) 145.
[23] A. T. T. Briggs, B. R. Butler, *J. Cryst. Growth 85* (1987) 535.
[24] T. F. Kuech, E. Veuhoff, B. S. Meyerson, *J. Cryst. Growth 68* (1984) 48.
[25] J. M. Boud, M. A. Fisher, D. Lancefield, A. R. Adams, E. J. Thrush, C. G. Cureton, *Inst. Phys. Conf. Series* No. 91, 1987, p. 801.
[26] See e.g. R. J. M. Griffiths in *Abstracts of 3rd European Workshop on MOVPE,* Montpellier, France, 5–7 June 1989, p. 16.
[27] R. W. Kaliski, C. R. Ho, D. G. McIntyre, M. Feng, K. B. Kim, R. Bean, K. Zznio, K. C. Hsieh, *J. Appl. Phys. 64* (1988) 1196.
[28] J. O. Williams, *Chemtronics 2* (1987) 43.
[29] H. M. Yates, J. O. Williams, *Appl. Phys. Lett. 51* (1987) 809.
[30] J. E. Potts, H. Cheng, S. Mohapatra, T. L. Smith, *J. Appl. Phys. 63* (1987) 333.
[31] A. H. Reddoch, D. J. Northcott, J. M. Park, J. O. Williams, unpublished results.
[32] P. Demeester, A. Ackart, M. Van Ackere, F. DePestel, C. Eckhout, Y. Grigase, D. Lootens, I. Moerman, G. Van den Bossche, R. Baets, M. Bottle, P. Van Daele, P. Lagasse, *Chemtronics 4* (1989) 44.
[33] M. A. diForte-Poisson, C. Brylinski, *Chemtronics 4* (1989) 3.
[34] P. L. Maurel, M. DeFour, D. Grattepain, F. Omnes, O. Acher, G. Timms, M. Razeghi, J. C. Portal, *Chemtronics 4* (1989) 40.
[35] i) S. K. Haywood, private communication. ii) S. K. Haywood, A. B. Henriques, D. F. Howell, N. J. Mason, R. J. Nicholas, P. J. Walker, *Inst. Phys. Conf. Ser. 91* (1988) 271.

[36] R. D. Dupuis, J. P. Van der Ziel, R. A. Logan, J. M. Brown, C. J. Pinzone, *Appl. Phys. Lett. 50* (1987) 407.
[37] R. D. Dupuis, J. C. Bean, J. M. Brown, A. T. Macrander, R. C. Miller, L. C. Hopkins, *J. Electron. Mater. 16* (1987) 69.
[38] J. W. Orton, *Chemtronics 3* (1988) 129.
[39] M. J. Kelly in M. J. Kelly, C. Weisbuch (Eds.): *The Physics and Fabrication of Microstructures and Microdevices*, Springer Verlag, Berlin 1986, p. 174.
[40] A. H. Cowley, B. L. Benac, J. G. Ekerdt, R. A. Jones, K. B. Kidd, J. Y. Lee, J. E. Miller, *J. Am. Chem. Soc. 110* (1988) 628.
[41] W. E. Johnson, L. A. Schlic, *Appl. Phys. Lett. 40(a)* (1982) 798.
[42] D. J. Ehrlich, J. Y. Tsao, C. O. Bozler, *J. Vac. Sci. Technol. 83 (1)* (1985) 1.
[43] S. D. Hersee, E. Barbier, R. Blondeau, *J. Cryst. Growth 77* (1986) 310.
[44] P. Demeester, P. Van Daele, R. Baets, *J. Appl. Phys. 63* (1988) 2284.
[45] A. Yoshikawa, A. Yamamoto, M. Hirose, T. Sugino, G. Kana, I. Teramoto, *IEEE J. Quantum Electron. QE-23 (6)* (1987) 725.
[46] M. D. Scott, J. R. Riffat, I. Griffith, J. I. Davies, A. C. Marshall, *J. Cryst. Growth 93* (1988) 820.
[47] B. Garrett, E. J. Thrush, *J. Cryst. Growth* (1989) in press.
[48] See e.g. *Chemtronics 2* (1987) 106–140.
[49] *MRS Bulletin xiv(i)* (1989) 20–67.
[50] H. Yamane, H. Kurosawa, H. Iwasaki, H. Masumoto, T. Hirai, N. Kobayshi, Y. Muto, *Jpn. J. Appl. Phys. 27 (7)* (1988) L1275.
[51] J. O. Wiliams, N. J. Dunhill, *Chemtronics 4* (1989) in press.
[52] C. J. Brierley, private communication.
[53] J. O. Williams, J. Simpson, unpublished observations.
[54] B. A. Joyce, *Adv. Mater. 1989*, This issue; *Angew. Chem. Int. Ed. Engl. Adv. Mater. 28* (1989) No. 8; *Angew. Chem. Adv. Mater. 101* (1989) No. 8.
[55] Taken from J. M. Rowell, *Sci. Am.* (Oct. 1986) p. 132.

Communications

Manuscripts intended for publication as communications should be sent to ADVANCED MATERIALS PO Box 101161, D-6940 Weinheim, FRG. Authors are requested to consult the "Instructions to Authors" which are reproduced in the January issue of the journal or are available from the editorial office on request.

Siloxane Copolymers with Laterally and Terminally Attached Mesogenic Side Chains**

By *G. W. Gray**, *J. S. Hill* and *D. Lacey*

In view of the demand for liquid crystal polymers of different types[1] with certain specific physical characteristics, many workers have considered how this could be met through synthesizing copolymers containing two or more terminally attached mesogenic side chains, and tuning the properties of the polymers by variation of the type and ratio of the side chains. In this way, using the smectic-depressing properties of a lateral methyl substituent, a nematic side-chain polysiloxane with a proportion (but only up to 32%) of terminal cyano-groups and positive dielectric anisotropy was first produced.[2]

Acrylate polymers containing mesogenic groups attached laterally to the backbone were first reported by *Finkelmann*,[3] and analogous polysiloxanes have since been reported by *Gray* et al.[4] and *Keller* et al.[5] These are predominantly nematic materials, and by synthesizing a series of novel siloxane copolymers containing varying amounts of terminally *and* laterally attached mesogenic groups, we now show that a further degree of flexibility is provided for the development of liquid crystal polymers with defined physical characteristics for applications in areas such as integrated optics,[6] optical storage,[1,7] gas liquid chromatography,[1] and NCAP displays,[8] e.g. nematic polysiloxanes containing 80–85% of cyanosubstituted side chains, and having a range of dielectric properties of technological interest.

Experimental

For the precursor of the *terminally* attached moiety we chose the alkene **1**, which gives a crystalline smectic homopolymer with relatively high melting and clearing points. Most laterally attached polysiloxanes which have been prepared to date are nematogenic and have a glass transition. We chose as the *lateral* comesogenic precursor the alkene **2** which has been prepared in our laboratories, and gives a typically low T_g, low T_{N-I} homopolymer.

The synthesis of those compounds using standard procedures is shown in scheme 1.

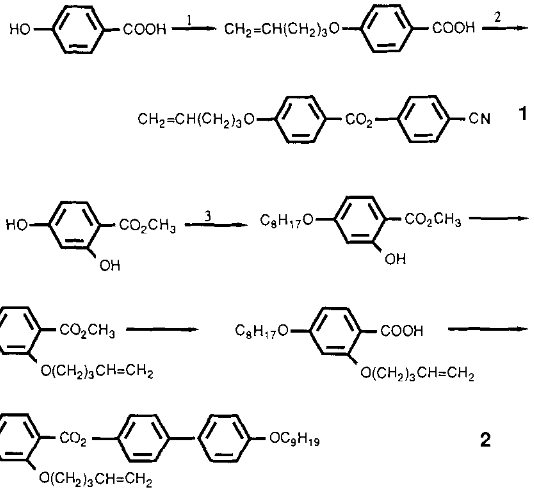

Scheme 1.

The copolymers were prepared by hydrosilylation of the alkenes in toluene at 70 °C for 18–24 h (Scheme 2), using poly(hydrogenmethylsiloxane) obtained from Wacker Chemie (DP $\sim$46, $\gamma \sim 2.2$); a 1.1 molar excess of the mixture of alkenes was used, with platinum divinyltetramethyl disiloxane as the catalyst. Purification was effected by repeated precipitation of the polymers from dichloromethane solution with 3:2 v:v methanol:ether, and subsequent centrifugation. The pure polymers were dried in vacuo in the isotropic state.

---

[*] Prof. G. W. Gray, Dr. J. S. Hill, Dr. D. Lacey
School of Chemistry, The University of Hull,
Hull, HU6 7RX (UK)

[**] The authors thank the Science and Engineering Research Council for financial support of the research of which this work was a part.